In Vivo 3D MRI Measurement of Tumour Volume in an Orthotopic Mouse Model of Prostate Cancer

Jie Ni, MBBS, PhD[1,2], Andre Bongers, PhD[3], Uphar Chamoli, PhD[4,5],
Joseph Bucci, MBBS, FRACP, FRANZCR[1,2],
Peter Graham, MBBS, FRANZCR[1,2], and Yong Li, MD, PhD[1,2,6]

Abstract

Prostate cancer (CaP) is the most commonly diagnosed cancer in males in western countries. Orthotopic implantation is considered as an ideal xenograft model for CaP study, and noninvasive measurement of tumor volume changes is important for monitoring responses to anticancer therapies. In this study, the T2-weighted fast spin echo sequence magnetic resonance imaging (MRI) was performed on a CaP orthotopic non-obese diabetic/severe combined immunodeficiency (NOD/SCID) mouse model weekly for 6 weeks post PC-3 CaP cell inoculation, and the fat signal was suppressed using a chemical shift-selective pulse. Subsequently, the MRI data were imported into the image processing software Avizo Standard and stacked into three-dimensional (3D) volumes. Our results demonstrate that MRI, combined with 3D reconstruction, is a feasible and sensitive method to assess tumor growth in a PC-3 orthotopic CaP mouse model and this established monitoring approach is promising for longitudinal observation of CaP xenograft development after anticancer therapy *in vivo*. Further investigation is needed to validate this protocol in a larger cohort of mice to generate enough statistical power.

Keywords

prostate cancer, animal model, magnetic resonance imaging

Introduction

Prostate cancer (CaP) is the most commonly diagnosed cancer and the second leading cause of cancer-related death in males in the United States in 2017.[1] To further facilitate the translation of scientific findings, reliable preclinical model systems that accurately mimic the clinical scenarios are needed. Orthotopic implantation is considered as an ideal xenograft model for more realistic modelling of the tumor microenvironment influence.[2] One major challenge for many preclinical studies to investigate CaP in preclinical models is the lack of reliable approaches to monitor tumor growth in a longitudinal fashion. Noninvasive prostatic tumor imaging constitutes a major step forward in terms of assessment of tumor growth and evaluation of the efficacy of cancer treatment.

[1] Cancer Care Centre, St George Hospital, Kogarah, New South Wales, Australia
[2] St George and Sutherland Clinical School, UNSW Sydney, New South Wales, Australia
[3] Biological Resource Imaging Laboratory, UNSW Sydney, New South Wales, Australia
[4] Spine Service, Department of Orthopaedic Surgery, St George and Sutherland Clinical School, UNSW Sydney, Kogarah, New South Wales, Australia
[5] School of Biomedical Engineering, University of Technology Sydney, Ultimo, New South Wales, Australia
[6] School of Basic Medical Sciences, Zhengzhou University, Henan, China

Corresponding Author:
Yong Li, Level 2, Research and Education Centre, St George Hospital, 4-10 South St, Kogarah, New South Wales 2217, Australia.
Email: y.li@unsw.edu.au

Specifically, magnetic resonance imaging (MRI) offers reliable visualization of soft tissues and thus has shown advantages as a means to better select patients for biopsy and identify lesions for biopsy in the clinical setting for CaP diagnosis. It is also useful in tumor staging and treatment response monitoring.

In preclinical CaP animal model imaging, MRI is thought to be the superior choice due to its high resolution and superior soft tissue contrast. Dedicated MRI pulse sequences allow for the identification of different structures based on tissue characteristics of the prostate gland or the tumor tissue.[3] Ravoori et al used T2-based Dixon "water only" sequence to clearly visualize the mouse prostate gland in young and old mice[4]; it was also reported by Mallett et al that MRI using the balanced steady-state free precession sequence could identify prostate tumors both anatomically and functionally.[5] In order to clearly detect extracapsular prostate tumor extension which is surrounded by the periprostatic fat, fat suppression techniques such as chemical shift-selective (CHESS) pulse have been developed to repress the signal from the fat.[6,7]

Compared to human prostate, mouse prostate gland has a larger anatomical variation and does not remain fixed, which makes it challenging to be identified.[8] Three-dimensional (3D) volumetric MRI has been used in various oncologic applications for tumor detection such as in central nervous and musculoskeletal systems.[9-11] The purpose of this study is to show the utility of a novel 2-dimensional (2D)-T2w fast spin echo (FSE) sequence combined with CHESS fat suppression to monitor prostate tumor growth in an orthotopic non-obese diabetic/severe combined immunodeficiency (NOD/SCID) mouse model and to assess the feasibility and accuracy of tumor volume measurement using 3D reconstruction from 2D slices. The results may have significant implications in monitoring treatment effects of CaP after different modalities in the preclinical study.

Materials and Methods

Cell Line and Cell Culture

The androgen-independent PC-3 CaP cell line was obtained from American Type Culture Collection (Rockville, Maryland) and cultured in Roswell Park Memorial Institute (RPMI) 1640 medium supplemented with 10% fetal bovine serum, 50 U/mL of penicillin, and 50 μg/mL of streptomycin, and maintained in a humidified incubator at 37°C and 5% CO_2. Subconfluent cells were harvested and centrifuged at 180 g for 5 minutes, followed by resuspension in the Dulbecco's phosphate-buffered saline (DPBS) for animal study.

Animal Model

Three male, 6 weeks old NOD/SCID mice (Animal Resources Centre, Western Australia, Australia) were housed under specific pathogen-free conditions and all experiments were performed in a laminar flow cabinet. Mice were kept at least 1 week before experimental manipulation. All mice were monitored daily and the weights were recorded at least twice a week.

Mice were anesthetized and placed in supine position. After a lower midline laparotomy incision, 50 μL DPBS suspension containing 1×10^6 PC-3 CaP cells were injected into the ventral prostatic lobe, followed by muscle layer and skin closures.[12] Starting from the first week after cell implantation, tumor progression was monitored weekly by MRI.

Magnetic Resonance Imaging Protocol

All imaging was performed using a 9.4-T Bruker BioSpec 94/20 Avance III micro-imaging system (Bruker, Ettlingen, Germany) equipped with BGA-12 S hyperpolarized (HP) gradients with maximum strength 660 mT/m and slew rate 4570 Tm/s and a 35-mm quadrature radiofrequency coil. Prior to imaging, animals were anesthetized in an induction chamber with 4% isoflurane/oxygen mixture (1 L/min). Animals were then transferred to the scanner animal bed and received 2% to 2.5% isoflurane at 0.8 L/min oxygen flow rate through a nose cone to maintain anesthesia during the scanning procedure. Respiratory motion was monitored during the imaging procedures using a pressure sensitive pad. Animal body temperature was maintained at 36°C by a temperature controlled circulating water warming blanket.

At each time point MR images were acquired in axial orientation. To minimize susceptibility artefacts and signal dephasing in the heterogenous abdominal region, we optimized a 2D FSE (TurboRARE) sequence. In contrast to gradient echo techniques which are commonly used in such studies,[5] the spin-echo-based method refocuses effects from static spin dephasing while still maintaining high temporal efficiency by using an echo train of refocusing pulses. The sequence was optimized for best T2 contrast and low artefacts (from susceptibility and fat shifts) specifically in the tissues inside and surrounding the prostate tumor while still maintaining high signal-to-nosie ratio (SNR) and good tumor delineation using the following general imaging parameters: Echo Time (TE) = 21 milliseconds, Repetition Time (TR) = 2177 milliseconds, Bandwidth (BW) = 80000 Hz, Echo Train Length (ETL) = 8, slice thickness = 500 mm, field of view 30 × 30 mm, matrix size 192 × 192, in-plane resolution 156 × 156 μm, 30 slices, and total acquisition time 11 minutes. The relatively short echo time was able to maintain good T2 contrast while reducing signal decay and susceptibility problems in our high field system in the heterogeneous pelvic region and therefore was able to maintain the most favorable contrast-to-noise ratio (CNR) around the prostate.

To minimize abdominal fat signals, we have used relatively high spectral BW as a compromise between signal and shift distance. The fat signal was additionally suppressed using a CHESS-based preparation scheme prior to the image readout. The suppression used a Gaussian saturation pulse with pulse duration of 1.957 milliseconds and BW of 1400 Hz. Signal was subsequently spoiled using a 130 mT gradient pulse applied in slice encoding direction for 2 milliseconds. Overall duration of fat saturation preparation was 5.2 milliseconds.
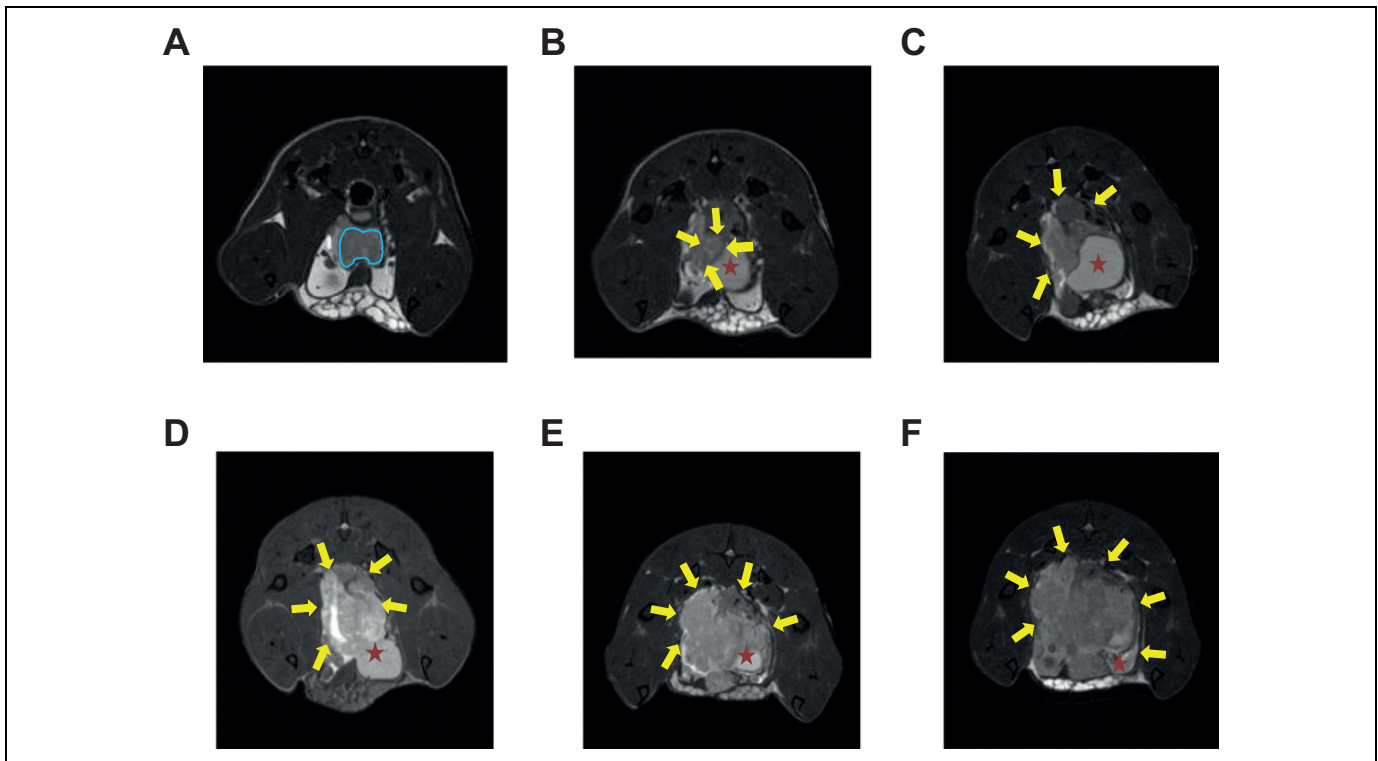
Figure 1. Representative MRI images of longitudinal tumor growth in the orthotopic mouse model. A-F, Images were acquired at 1,2,3,4,5, and 6 week(s) post CaP cell inoculation, respectively. A-D were acquired from mouse 1, and E, F were acquired from mouse 2. Prostate cancer (CaP) tumorigenesis as early as 1 week after cell inoculation could be detected, and CaP tumor is clearly delineated from surrounding anatomies. *Blue line* delineates the prostate gland; *Yellow arrow* indicates prostate tumor boundaries; *red star* indicates the urinary bladder. CaP, prostate cancer; MRI, magnetic resonance imaging.

Three-Dimensional Reconstruction and Tumour Volume Measurements

MR data from the weekly scanning was converted from Bruker proprietary (2dseq) format into 30 DICOM (Digital Imaging and Communications in Medicine) slices per animal and time point. The MR data were then imported into the image processing software Avizo Standard (version 8.1; FEI Visualization Sciences Group, Hillsboro, Oregon) and stacked into a 3D volume within the software. The MR images were segmented by manually delineating the hyperintense prostate area on each 2D slice and pixels inside the prostate were assigned to a color-coded material mask. The volume of the tumor was estimated by adding up the individual voxel volumes inside the tumor while taking partial volume effects on the boundaries of the surface into account using the Material Statistics tool in Avizo Standard. From this the material mask, a 3D surface model reconstruction of the tumor was generated using the SurfaceGen tool in Avizo, enclosing all the segmented voxels.

Tumor Growth Curve and Statistical Analysis

Tumor growth was investigated by calcualting tumor volumes for each longtitudinal time point and then fitting an exponential growth model by nonlinear regression using GraphPad Prism 7 package (GraphPad, California). Value of $P < 0.05$ is considered statistically significant. Upon sacrifice, primary prostate tumors were harvested from the mice and measured by a calliper. The gross tumor volumes were calculated as follows: length $\times$ width $\times$ height $\times$ 0.52 (in millimeters). Pearson correlation coefficients were used to assess the degree of correlation of two cohorts of data. Agreement of the MRI and gross pathology volumetric measurements were assessed using Bland-Altman analysis.

Results

T2w MRI Is a Useful tool to Monitor Prostate Tumor Growth in the Orthotopic Mouse Model

In this study, the prostate gland and the tumor were easily visualized in MR images. It was found the prostate gland was discernible by its position and shape at the beginning, and was engulfed within the tumor and became indistinguishable as tumor grow at late stages.

In the images from early time points, the prostate gland was found to be visible as a darker tissue whereas the tumor presents as a hyper-intense lesion (Figure 1). We found substantial signal heterogeneities within the tumor. We attribute the hyper-intense regions to regions with relative high water content, possibly caused by edema, whereas dark regions are
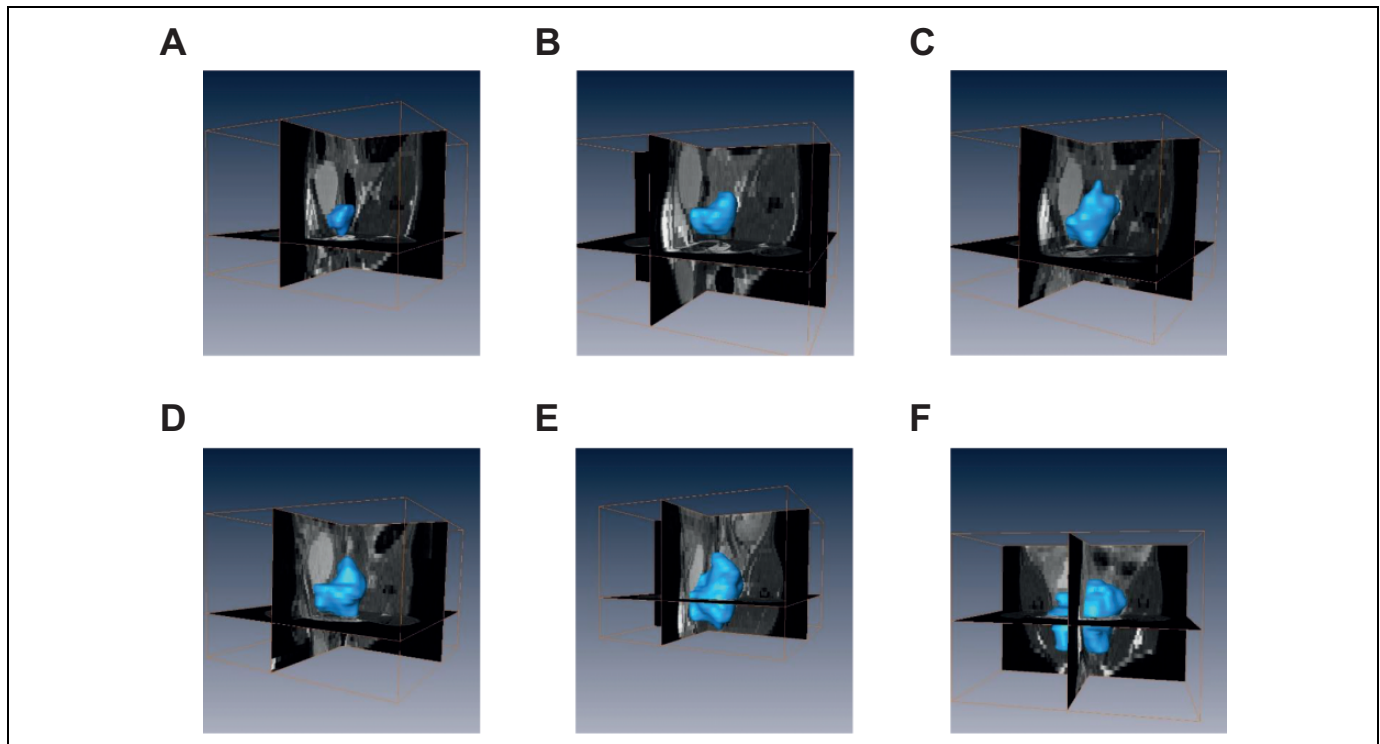
Figure 2. Representative 3D reconstructed MRI images of longitudinal tumor growth in the orthotopic mouse model. A-F, Using Avizo Standard software, MRI scan slices acquired from the same mouse were reconstructed into 3D (outlined by blue surface) at 6 different time points, respectively. 3D, three-dimensional; MRI, magnetic resonance imaging.

presumably highly vascularized regions or necrotic regions with components of hemorrhage. Compartmentation was also noticed in the tumor region only at the late stages but not at early stages (Figure 1E and F).

Longitudinal Imaging of Tumor Growth

Figure 1A-F shows the representative 2D images of 6 time points (1-6 weeks post cell inoculation, respectively). The tumor can be distinguished from the 2D-MRI image as early as 1 week post cell injection. Image stacks were loaded into the Avizo Standard software and reconstructed. Figure 2A-F illustrates representative 3D rendering of the tumors from the corresponding mouse in Figure 1, respectively.

Longitudinal tumor volume measurements were obtained from all 3 mice and were plotted in Figure 3A. The results indicate that the exponential growth functions fit the volume data well ($r^2 = 0.968, 0.966, 0.967$, respectively).

### Agreement of MRI and Gross Pathology Volume Measurements

Paired volumetric measurements obtained from 3D reconstruction and the xenografts harvested at the end of the experiment from 3 mice are plotted in Figure 3B. With linear regression, Pearson correlation coefficient is $r = 0.92$, but the P value is 0.25, indicating the correlation is not statistically significant.

The Bland-Altman scatter plot (Figure 3C) showed a close agreement between MRI and xenograft measurements. The difference was plotted against the average, and the standard deviation of the difference (bias) was 6.25 mm^3, which was quite small compared with the true volume of the tumors.

Discussion

One of the major obstacles that is still hampering the widespread use of CaP orthotopic xenograft models is the challenge of reliably imaging the orthotopic tumor growth and metastasis. Ideally, a small-animal preclinical imaging technology should be sensitive to detect the tumors, acquire high-quality images rapidly, easy to maintain, and harmless to the animals.[13]

The most frequently-used technique to monitor tumor growth in orthotopic xenograft models of CaP is bioluminescence imaging (BLI).[14] Prostate cancer xenograft models were among the first models demonstrating exciting BLI results.[15,16] Bioluminescence imaging is fast, easy, and relatively inexpensive but also comes along with severe drawbacks. Specifically, the method is restricted to luciferase-transfected tumor cells, which always requires genetic modification. BLI has inherently very low spatial resolution, restricting it to 2D projection acquisitions and the quantification of the tumor progression is very difficult due to light scattering and poor spatial resolution.
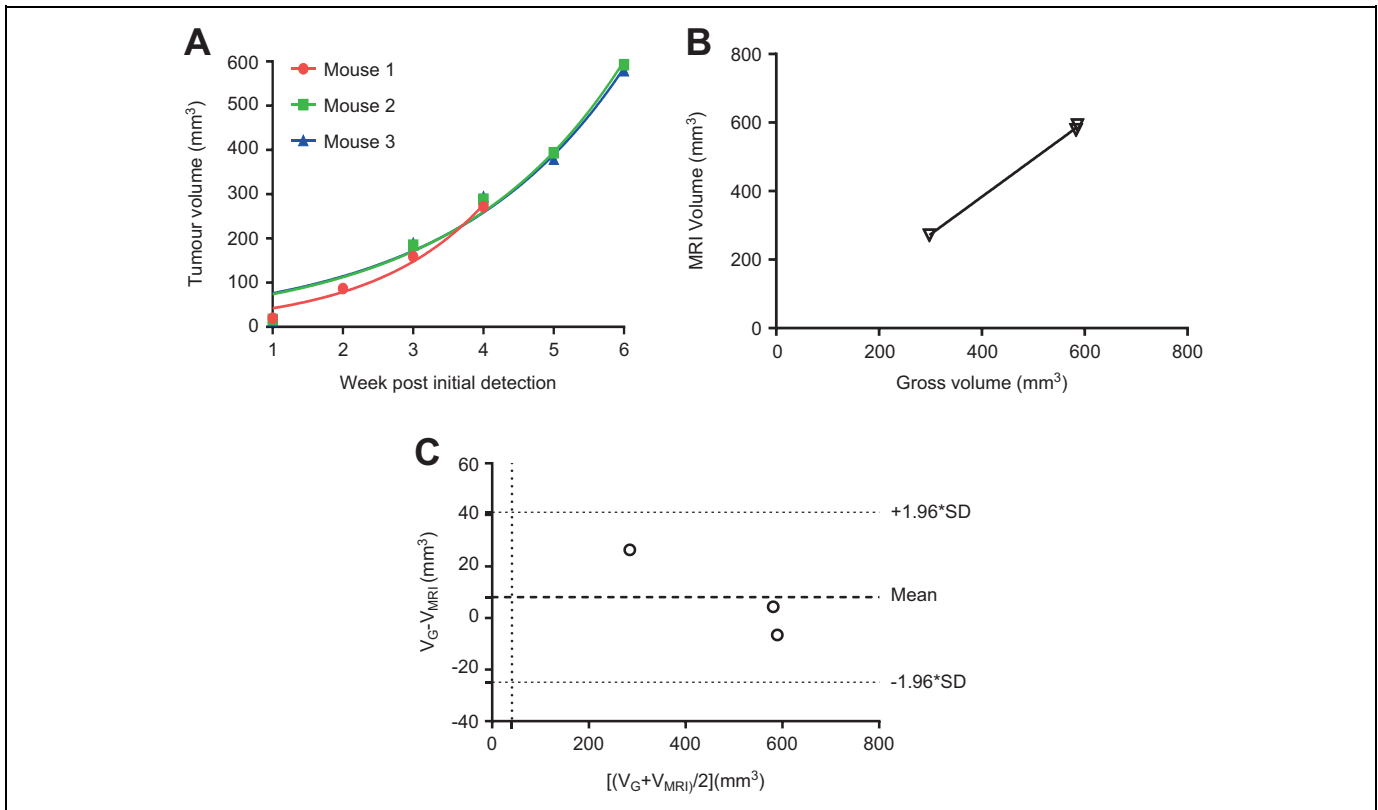
Figure 3. Exponential growth curves for longitudinal 3D volumetric measurements, correlation and agreement of 3D MRI with gross pathology measurements. A, Three-dimensional MRI prostate tumor volumes from the 3 mice were plotted against time, with fitted exponential growth curves, $r^2 = 0.968$, 0.966, and 0.967, respectively. B, Correlation of 3 paired tumor volumes measured by 3D MRI and gross pathology was demonstrated by linear regression. Pearson $r = 0.92$, $P = .24$. C, Good agreement between 3D MRI and gross pathology measurements were plotted and analyzed using Bland-Altman analysis. 3D, three-dimensional; MRI, magnetic resonance imaging; SD, standard deviation.

Ultrasound is also widely used in the detection of tumor growth in CaP orthotopic xenograft models but exhibits limited image quality and exact definition of tumor volume remains difficult. In a previous parallel study, our group has demonstrated that 3D ultrasound is a useful, economical, and sensitive method to monitor longitudinal tumor growth in the orthotopic CaP mouse model,[13] allowing for high spatial resolution and contrast with fast and uncomplicated protocols. However, ultrasound faces challenges due to small penetration depth, ultrasonic scattering and susceptibility of acoustic impedance barriers in tissues, limiting the visibility of specific structures.

MRI meets all criteria listed above and is a powerful and useful imaging modality and has been used extensively for detecting and modelling CaP in humans and preclinical applications,[17,18] such as early detection of CaP, active surveillance for low-risk patients, as well as targeted biopsies of the prostate in clinical settings.[19] Magnetic resonance imaging has also been shown to be useful in the detection of preclinical CaP mouse xenografts models. Previous studies have used both gradient echo (GRE)-based and spin-echo-based MRI methods to detect and delineate CaP. Using balanced steady-state free precession sequences, Mallett et al showed that GRE-based MRI can successfully monitor tumor growth in orthotopic PC-3M tumors,[5] and Li et al have studied visibility of CaP,

with the finding that visibility in these methods depends on gene expression in the tumor.[3] Previously, spin-echo-based sequences have been used which (due to the refocusing of static inhomogeneities) generally provide better stability in abdominal regions but often come with the downside of long scan times. Ravoori et al used T2-based Dixon water-only sequences to depict the mouse prostate in young and old nude mice at 4.7 and 7 T.[4] Song et al demonstrated that T2-diffusion-weighted imaging (DWI) could detect tumors <1 mm in diameter and distinguish benign and malignant prostatic tissue in a CR2-TAg transgenic mouse model.[20] Due to the single spin echo acquisitions, such methods take a relatively long time; in this study, we have adapted and optimized a T2w FSE sequence to monitor the intraprostatic tumor growth in a PC-3 CaP mouse xenograft model. The use of an FSE sequence circumvents the sensitivity to the very abundant susceptibility variations in the abdomen that GRE-based methods commonly face while still maintaining high SNR and relatively short acquisition times. Using relatively short TE in conjunction with fat suppression allowed us to benefit from the high stability of spin echo methods in relatively quick scans of ~10 minutes while maintaining high stability. Our results indicate that MRI with T2w FSE sequence is able to detect an intraprostatic tumor as early as 1 week post cell inoculation, and also showed a good agreement

between MRI measurement and gross pathology. One limitation is that only 3 mice were tested in the study, which is not enough for statistical power to reveal significant correlation.

Our imaging protocol also combined a CHESS pulse with T2w FSE to eliminate the fat signal in the prostate region. To obtain good fat suppression particularly when imaging abdominal regions in high field scanners as ours, it is better to optimize field homogeneity across the region of interest to enable on resonance saturation of the fat protons in all regions. To achieve this, we optimized main magnetic field homogeneity in the tumor region using a field map–based shimming to the second order prior to the actual image acquisition. This approach was able to largely eliminate inhomogeneities and optimize fat saturation in the tumor region. Due to susceptibility variations in the abdomen (eg, from air, tissue and water boundaries in intestinum and bladder) which are specifically strong in high field scanners as ours, some regions outside the region of interest remained off-resonant to the CHESS pulse, deteriorating fat saturation outside these regions, which didn't affect our analysis.

Additionally, MRI allows for the measurement of parameters other than volume: Mallett et al showed that hyperpolarized (HP) ^{13}C magnetic resonance spectroscopic imaging (MRSI) has the potential to assess tumor metabolism and necrosis of orthotopic xenografts in a CaP nude mice model.[5] Using the same technique, Aggarwal et al demonstrated that HP 1-[^{13}C]-pyruvate MRSI could detect the metabolic changes within the prostate tumor as early as 6 weeks after the initiation of androgen deprivation therapy, while there was no such a response that could be ascertained using standard MRI.[21]

Taken together, we have successfully demonstrated that MRI combined with 3D reconstruction is a feasible and sensitive method to monitor tumor growth in a PC-3 orthotopic CaP mouse model. Further investigation is needed to validate this protocol in a larger cohort of mice to generate enough statistical power and to combine molecular imaging technologies to supplement the current MRI protocols.

Authors' Note

UNSW Sydney Animal Care and Ethics Committee approved the experimental procedures (approval number ACEC 14/46A). All animal housing and experiments were conducted in strict accordance with the UNSW Animal Research Ethics Procedure, Australian Code for the Care and Use of Animals for Scientific Purposes (8th edition, 2013), and Animal Research Act 1985.

Declaration of Conflicting Interests

The author(s) declared no potential conflicts of interest with respect to the research, authorship, and/or publication of this article.

Funding

ORCID iD

Yong Li https://orcid.org/0000-0002-8910-9787

References

1. Siegel RL, Miller KD, Jemal A. Cancer Statistics, 2017. *CA Cancer J Clin*. 2017;67(1):7-30.
2. Radiloff DR, Rinella ES, Threadgill DW. Modeling cancer patient populations in mice: complex genetic and environmental factors. *Drug Discov Today Dis Models*. 2008;4(2): 83-88.
3. Li P, You S, Nguyen C, et al. Genes involved in prostate cancer progression determine MRI visibility. *Theranostics*. 2018;8(7): 1752-1765.
4. Ravoori M, Duggal J, Gagea M, et al. Visualizing the prostate gland by MR imaging in young and old mice. *PLoS One*. 2013; 8(3):e55746.
5. Mallett CL, Lim H, Thind K, et al. Longitudinal anatomical and metabolic MRI characterization of orthotopic xenograft prostate tumors in nude mice. *J Magn Reson Imaging*. 2014;40(4): 848-856.
6. Frahm J, Haase A, Hanicke W, Matthaei D, Bomsdorf H, Helzel T. Chemical shift selective MR imaging using a whole-body magnet. *Radiology*. 1985;156(2):441-444.
7. Nastiuk KL, Liu H, Hamamura M, Muftuler LT, Nalcioglu O, Krolewski JJ. In vivo MRI volumetric measurement of prostate regression and growth in mice. *BMC Urol*. 2007;7:12.
8. Roy-Burman P, Wu H, Powell WC, Hagenkord J, Cohen MB. Genetically defined mouse models that mimic natural aspects of human prostate cancer development. *Endocr Relat Cancer*. 2004; 11(2):225-254.
9. Ahlawat S, Morris C, Fayad LM. Three-dimensional volumetric MRI with isotropic resolution: improved speed of acquisition, spatial resolution and assessment of lesion conspicuity in patients with recurrent soft tissue sarcoma. *Skeletal Radiol*. 2016;45(5): 645-652.
10. Kralik SF, O'Neill DP, Kamer AP, Rodriguez E, Ho CY. Radiological diagnosis of drop metastases from paediatric brain tumours using combination of 2D and 3D MRI sequences. *Clin Radiol*. 2017;72(10):902.e913-902.e919.
11. Lindberg K, Kouti A, Ziegelitz D, Hallén T, Skoglund T, Farahmand D. Three-dimensional volumetric segmentation of pituitary tumors: assessment of inter-rater agreement and comparison with conventional geometric equations. *J Neurol Surg B Skull Base*. 2018;79(5):475-481.
12. Li Y, Song E, Abbas Rizvi SM, et al. Inhibition of micrometastatic prostate cancer cell spread in animal models by 213Bilabeled multiple targeted alpha radioimmunoconjugates. *Clin Cancer Res*. 2009;15(3):865-875.
13. Ni J, Cozzi P, Hung TT, Hao J, Graham P, Li Y. Monitoring prostate tumor growth in an orthotopic mouse model using three-dimensional ultrasound imaging technique. *Transl Oncol*. 2016;9(1):41-45.
14. Linxweiler J, Korbel C, Muller A, et al. A novel mouse model of human prostate cancer to study intraprostatic tumor growth and

the development of lymph node metastases. *Prostate*. 2018;78(9): 664-675.

15. Iyer M. Two-step transcriptional amplification as a method for imaging. *PNAS*. 2001;98(25):14595-14600.

16. El Hilali N, Rubio N, Martinez-Villacampa M, Blanco J. Combined noninvasive imaging and luminometric quantification of luciferase-labeled human prostate tumors and metastases. *Lab Invest*. 2002;82(11):1563-1571.

17. Bourne RM, Bongers A, Chatterjee A, Sved P, Watson G. Diffusion anisotropy in fresh and fixed prostate tissue ex vivo. *Magn Reson Med*. 2016;76(2):626-634.

18. Bourne R, Liang S, Panagiotaki E, Bongers A, Sved P, Watson G. Measurement and modeling of diffusion time dependence of apparent diffusion coefficient and fractional anisotropy in prostate tissue ex vivo. *NMR Biomed*. 2017;30(10):e3751.

19. Pedler K, Kitzing YX, Varol C, Arianayagam M. The current status of MRI in prostate cancer. *Aust Fam Physician*. 2015; 44(4):225-230.

20. Song SK, Qu Z, Garabedian EM, Gordon JI, Milbrandt J, Ackerman JJ. Improved magnetic resonance imaging detection of prostate cancer in a transgenic mouse model. *Cancer Res*. 2002;62(5): 1555-1558.

21. Aggarwal R, Vigneron DB, Kurhanewicz J. Hyperpolarized 1-[(13)C]-pyruvate magnetic resonance imaging detects an early metabolic response to androgen ablation therapy in prostate cancer. *Eur Urol*. 2017;72(6):1028-1029.